

Article

Simulation, Fuzzy Analysis and Development of ZnO Nanostructure-based Piezoelectric MEMS Energy Harvester

Basit Ali ¹, Muhammad Waseem Ashraf ^{1,*} and Shahzadi Tayyaba ²

¹ Department of Physics (Electronics), GC University, Lahore 54000, Pakistan; basit_nano@yahoo.com

² Department of Computer Engineering, The University of Lahore, Lahore 54000, Pakistan; Shahzadi.Tayyaba@hotmail.com

* Correspondence: dr.waseem@gcu.edu.pk

Received: 17 January 2019; Accepted: 27 February 2019; Published: 28 February 2019



Abstract: Fuzzy logic-based control systems are widely used in various fields like home appliances, medical instruments, automobiles, textile machinery, agriculture equipment and aviation for process control and data analysis. Fuzzy logic technique has shown great potential to solve the complex problems of physical world due to similarity with human understanding. Its advancements have gained widespread attention in different research areas. In several cases, it is very suitable for electronic devices which need to be precisely self-powered. In this work, an ANSYS-based simulation, fuzzy analysis, development and testing of a microelectromechanical system (MEMS)-based energy harvester have been presented. Zinc oxide (ZnO) nano rods were synthesized on an anodic aluminum oxide (AAO) template to form the MEMS energy harvester and study the effect of energy generation by applying force. The power of 5.16 nano Watts has been obtained by taking the numerical value of voltage (V_{oc}) and current (I_{sc}) as 3.16 mV and 0.985 μ A respectively using fuzzy logic tool. Experimental testing of the harvester shows that the range of V_{oc} is 3–6.4 mV and I_{sc} is 0.45–1.5 μ A. The results depict that this device can be used for touch screens to generate energy that can be further utilized for charging smart devices.

Keywords: anodic aluminum oxide; fuzzy logic; piezoelectric harvester; ZnO nano-rods

1. Introduction

Energy harvesting utilizes energy sources like surrounding temperature, pulsation, the flow of air, solar power, thermal energy, wind energy and piezoelectric sources. Harvested energy can be analyzed using the fuzzy logic technique. The fuzzy approach is versatile and authentic. It is a method through which the limitations of various systems can be improved significantly. Fuzzy systems are rule-based, which depends on the real understanding of the worker [1]. Using such technology for the betterment of human life is a considerable research topic nowadays. Among various emerging devices, smart energy harvesters have achieved enormous attention. These systems are mainly comprised of piezo material. Microelectromechanical (MEMS) energy harvesting provides a platform to enhance system capabilities. Sensors are a significant element for monitoring and controlling vast amounts of real-time and remote data. These sensors are mainly used for light, weather, humidity and temperature measurements. However, the piezoelectric sensors are mostly used to detect mechanical energy (in the form of pressure, force, or vibration) applied to a material that can be further converted to electrical energy [2]. This mechanism of generation of electrical energy can be further utilized in touchpad and cell-phone charging, smart communication devices, laptops and tablets. Voltage and current are the main parameters that need to be optimized during the development of the energy harvester.

The deviations of these constraints are based on numerous important factors, and one of them includes the physical properties of the material. Zinc oxide (ZnO) is the most common material that has been used for the synthesis of nanostructures to develop the energy harvester. Variations of current and voltage for ZnO nanostructures on various substrates are given in Table 1.

Table 1. Variations of voltage and current for a ZnO nano-structures-based energy harvester.

References	Material	Deposition Technique	Simulation Technique	Substrate	Diameter (nm)	Length (μm)	Voltage (mV)	Current (μA)
Opuko 2015 [3]	ZnO nano-wires	Hydrothermal	Custom build test bench	Au/Ti-PEN	115 ± 64	0.97 ± 0.38	22	-
Salman Ahmed khan 2015 [4]	ZnO Micro-wires	Top down lithography	finite Element	AAO template -p type Si wafer	50–65	6–9	4–6	0.5–1
Liao 2014 [5]	ZnO nanowires	Hydrothermal	-	Carbon Fiber	~200	~2	18	35
Qui 2012 [6]	ZnO nano-rods	Hydrothermal	ZPNG	Common paper	100–200	4	10	0.1
Riaz 2010 [7]	ZnO nano-wires array	VLS	finite Element	n-Si	50–200	1–4	30–35	-
Zhu 2010 [8]	ZnO Nano-wires Array	PVD	HONG	Si Substrate	~200	~50	20–30	1.07
Riaz 2010 [7]	ZnO nano-wires array	ACG	finite Element	n-Si	50–200	1–4	5	-
Pu Xian 2007 [9]	ZnO nano-wires	Synthetic Chemical Approach	-	Plastic Substrate	100–350	~1	45	-
Ou 2016 [10]	Zinc Oxide nano-wires	Template assisted Hydro-thermal	Vibrational energy harvesting system	Nano-porous poly carbonate template	240 ± 40	8.4 ± 2.1	-	-

When stress is exerted on a material along certain planes then electric voltage is produced. The mechanism behind the generation of voltage is the dislocation of the center of gravity of the positive and negative charges [11]. This movement of the charge produces dipole movement which results into the polarization of the material that can be measured as the voltage across the terminals [12] as shown in Figure 1.

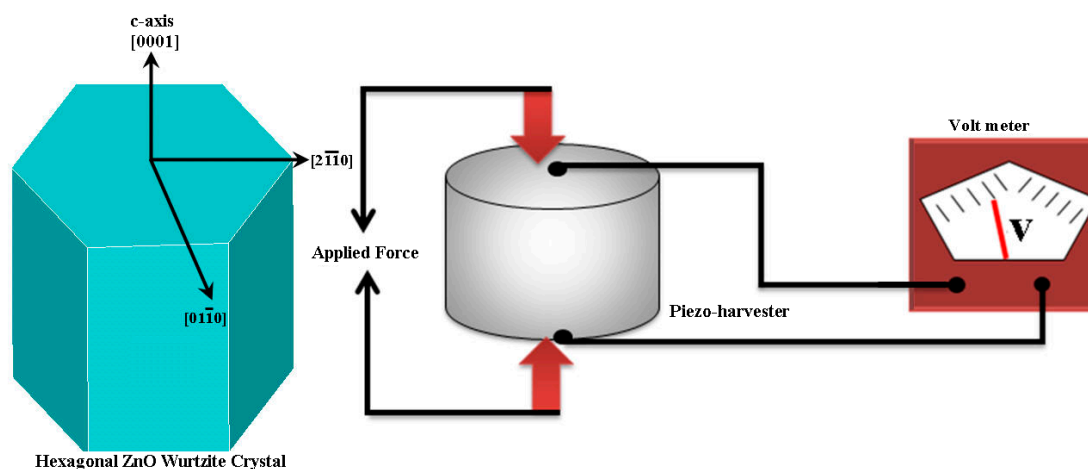


Figure 1. The basic working principle of a piezoelectric harvester.

By applying mechanical stress to a particular crystal, the electrical charge appeared. Piezoelectricity generation is actually a material property [13]. It is widely used with piezoelectric materials like Lead Zirconate Titanate and ZnO nanostructures. ZnO nanostructures have gained considerable attention due to their low cost [14], wider band-gap (i.e, 3.37 eV), and competent excitation emission at ambient temperatures because of the large exciton bonding energy and immense pyroelectric and piezoelectric properties [15]. Due to the superior piezoelectric properties of ZnO nano-rods and wires [16,17], stress applied to the length of nano-wire will result in a flow of electric current [18]. Previously, ZnO nano rods and wire-based structures have been deposited on a huge variety of substrates, including glass, silicon, aluminum, textile fabric, paper, carbon fiber, aluminum oxide, plastic, polymer [19]. Various techniques are used to sensitize nano-rods/wires, including aqueous solution [20], hydrothermal growth [21], and advanced techniques [22] like PVD, top-down lithography, and seedless growth [23].

Simulation is a good idea before the fabrication of an actual device and always leads to cost reduction. Various languages and software have been used for simulation, and among them, MATLAB and ANSYS are very good for simulations. It has been observed that by utilizing fuzzy tools and systems, improved results were obtained. These systems are arrangements of multi-valued logic 0 and 1 integers. Many researchers have done wonderful work by applying fuzzy simulations [24–27]. Many researchers use the fuzzy logic controller technique in designing energy storage systems by using a fuzzy proportional integral derivative (PID) controller. The control performance of the fuzzy PID has been verified for numerous working conditions by using the PSCAD/EMTDC simulating method [28]. In another research article, the momentary transient response and power are confirmed by the simulation and experiment [29]. It is reported that the asymmetrical MPPT algorithm for photovoltaic systems used the fuzzy logic controller MPPT method, and transient time and trailing accuracy were enhanced by 42.8% and 0.06%, separately [30]. In analyzing a real-time Simulink, the suggested charging stratagem helped complete the battery recharging in 9.76% less time than the CC/CV technique [31]. In developing a charging method, the proposed technique leads to 98.6% smallest cost for homes, and therefore it achieved the lowermost normal expenditures with the use of a fuzzy controller [32]. Fuzzy logic based energy management strategy was reported [33]. ANSYS was used to study piezoelectric energy harvester systems [34–37].

The software COMSOL was used in the simulation of the piezoelectric energy harvesting system. The assessment of three piezoelectric materials, PZT-5H, PMN-0.33%Pt, and PVDF was studied with a frequency of 153 Hz by using COMSOL [38]. In infrared solar energy collection, COMSOL simulation was used, which proved that the changed electric field in curved nano-antennas was greater than that in dipole and bow-tie nano-antennas [39]. ABAQUS software was used in the study of the resonant system in energy harvesting applications. This research has revealed a resonant reaction appropriate for combining piezoelectric material for energy harvesting [40]. For energy harvesting using MEMS devices in a non-linear system, the FE simulation of the energy harvester was directed with ABAQUS, and good results were perceived between both analytical and numerical simulations [41]. The software CATIA was also used in speed bumps for the mechanical energy harvesting method, which was a novel technique for improving the mechanical energy transformation with pulsed energy [42].

CATIA simulation was also used in the study of electrical and motorized models made for the evaluation of the quantity of recovered energy [43]. Among all the techniques, fuzzy logic methods are the most accurate and reliable. Fuzzy systems are used in many areas like aerospace, automotive, defense, electronics, control of automatic exposure in video cameras, humidity in a clean rooms, air conditioning systems, washing machine timing, microwave ovens, vacuum cleaners, finance, industrial, manufacturing, marine, medical, medical diagnostic support system, control of arterial pressure during anesthesia, multivariable control of anesthesia, radiology diagnoses, fuzzy inference diagnosis of diabetes and prostate cancer, securities, transportation, automatic underground train operation, train schedule control, railway acceleration, and braking and stopping systems. On the other hand, a 3D cad simulator like ANSYS is also a powerful tool for performing structural, fluid, thermal, electric, piezoelectric, magnetic, etc. analysis. In this work, the authors have designed a

system for the generation of current for smart MEMS energy harvesters. Fabrication and testing of the device are also performed. ZnO nano-rods on an anodized aluminum oxide template using were synthesized using a self-designed chemical bath deposition setup. Before fabrication, the structural simulation of the AAO template was performed to check the suitability of the template for the MEMS energy harvester. These results were also tested and verified by using fuzzy simulation. Anodized aluminum oxide is a widely used hexagonal closed pack nanostructure produced from Aluminum. It has wide applications in the field of chemical and bio-sensing, with photonic cell culturing owing to its high pore density and nano-porous configuration. Self-assembly is generally used to sensitize such porous structures.

2. ANSYS Simulation

The ANSYS Workbench has been used for the structural analysis of an anodic aluminum oxide nano-porous template. The strength of the AAO template has been examined because this template has been used as a base of the piezoelectric MEMS energy harvester. This was done in order to find out how much load this structure can bear before disintegrating. It also has conducting properties and it can serve as a part of an electrode. In the structural analysis, a template with a diameter of 20 mm, a thickness of 80 μm , and a pore diameter of 70 nm has been generated in the design modeler. After meshing the 3D structure, the analysis was set up by applying the boundary conditions like fixing the bottom of the template and applying the force of 3 μN on top of the surface. Then, the simulation was run, the solution was converged, and results were analyzed. The results of total deformation, stress intensity, and strain intensity tests have been studied. The 3D model geometry and meshed design are shown in Figure 2.

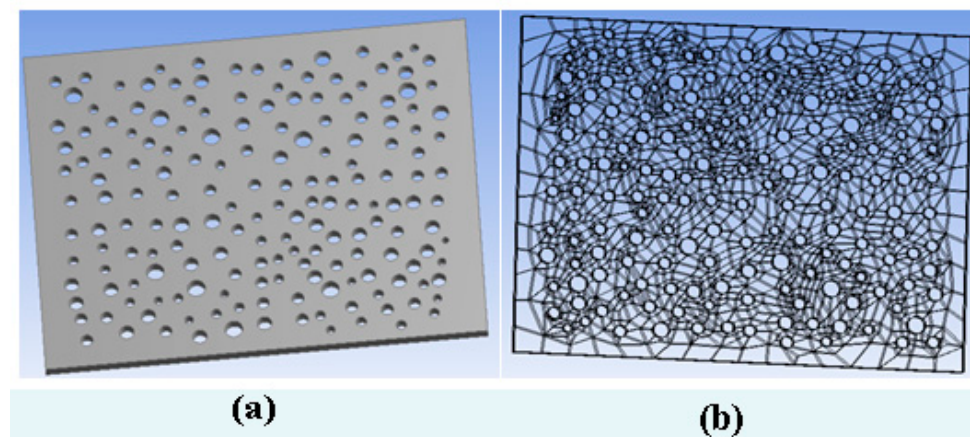


Figure 2. (a) Model in the design modeler; (b) the meshed model in mesh analysis

Meshing is a compulsory part of the simulation in ANSYS so that the loads are uniformly distributed around the geometry to obtain the real time results. The results of total deformation, strain intensity, and stress intensity were obtained and analyzed to check the mechanical properties, and these are shown in Figure 3.

By increasingly applying force on the nanoporous anodized aluminum oxide template, the rate of applied stress increases, which can be seen in Figure 4.

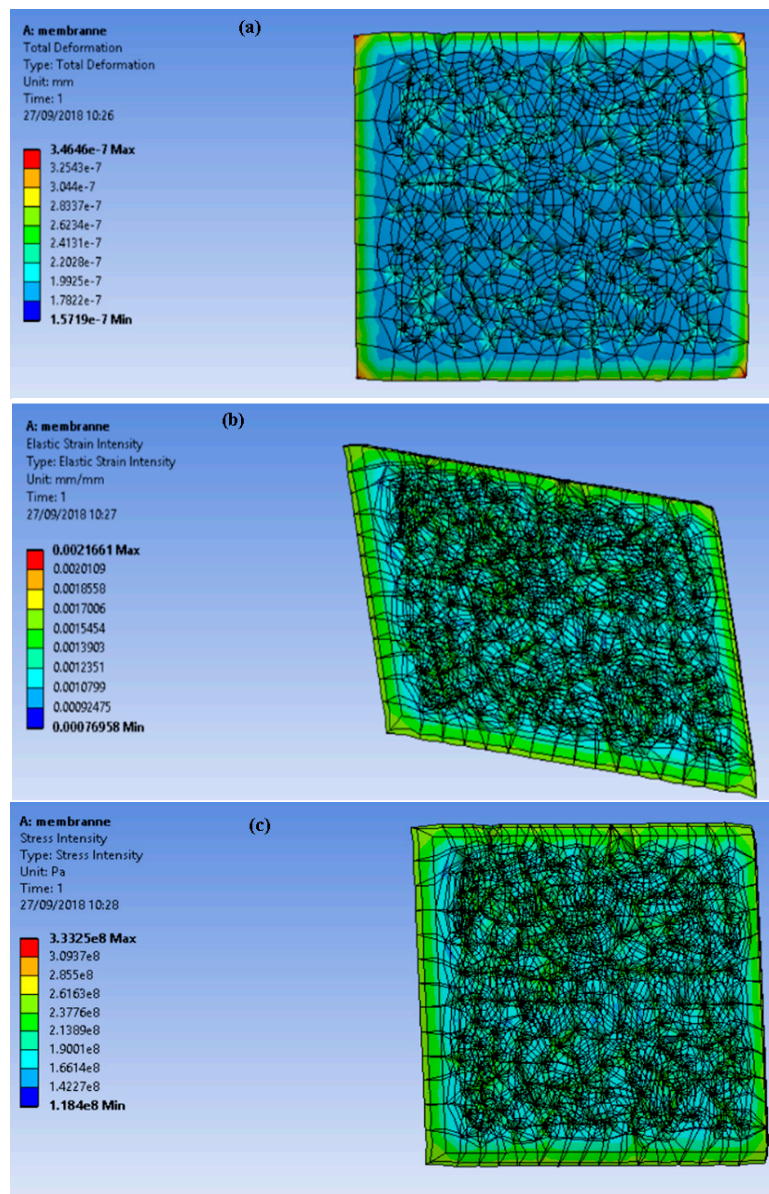


Figure 3. (a) Total deformation; (b) strain intensity; (c) stress intensity.

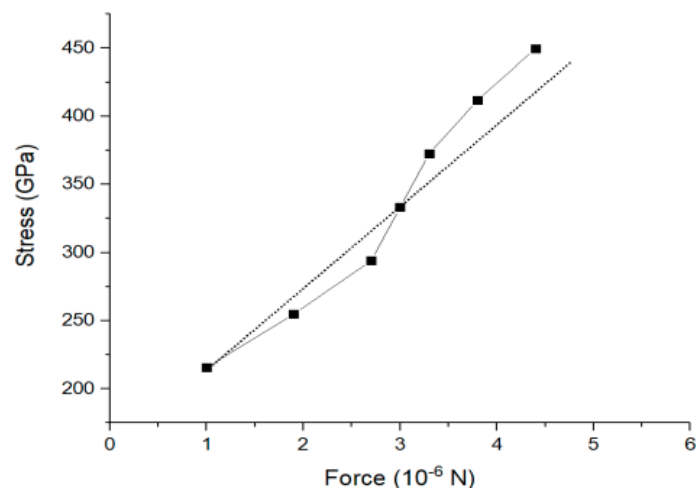


Figure 4. Graph of the relationship between stress and force.

It has been observed that with increases in applied force from 1.0 μN –3.8 μN , the applied stress on the nanoporous anodized aluminum oxide template has been increased from 200 GPa–450 GPa, as shown in Figure 5.

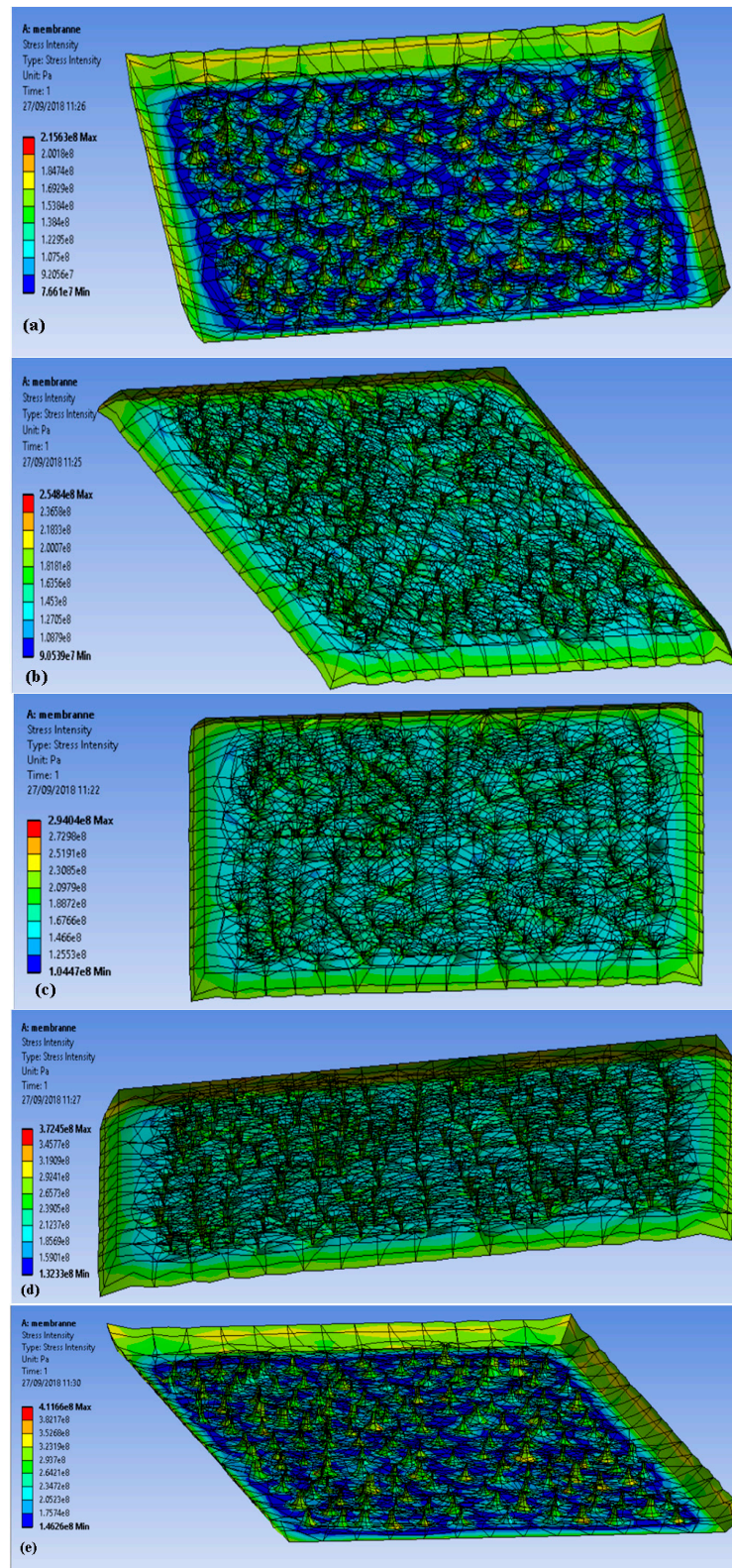


Figure 5. The stress intensity legend for the forces of (a)1.0 μN ; (b) 1.9 μN ; (c) 2.7 μN ; (d) 3.3 μN ; and (e) 3.8 μN .

Structural analysis shows that all the values are under the limits of the elastic modulus. After the ANSYS simulation, the fuzzy simulation is carried out for the calculation of power, with voltage and current as inputs. ANSYS is used only for the structural simulation to foresee the mechanical properties before fabrication of the nanostructure on the AAO substrate. It has been observed during simulation that the AAO template can be used as a substrate. A simulation of the fuzzy logic is presented in the next section. It has been performed for the estimation of power and efficiency.

3. Fuzzy Simulation

Fuzzy conditions are very close to ideal conditions and are found to be more accurate. They can provide thousands of infinite values between zero and one. Therefore, they are more dependable. In the literature, it is found that the fuzzy logic has been used in many appliances like blood pressure apparatuses, glucometers, washing machines, dryers, air conditioners, etc. Therefore, fuzzy logic has been used to estimate the power and efficiency of the MEMS energy harvester. In this fuzzy logic simulation, the energy harvester fuzzy logic controller (EHFLC) is designed in the fuzzy logic MATLAB toolbox. The input parameters are voltage and current, while the outputs are power and efficiency. EHFLC is shown in Figure 6 below.

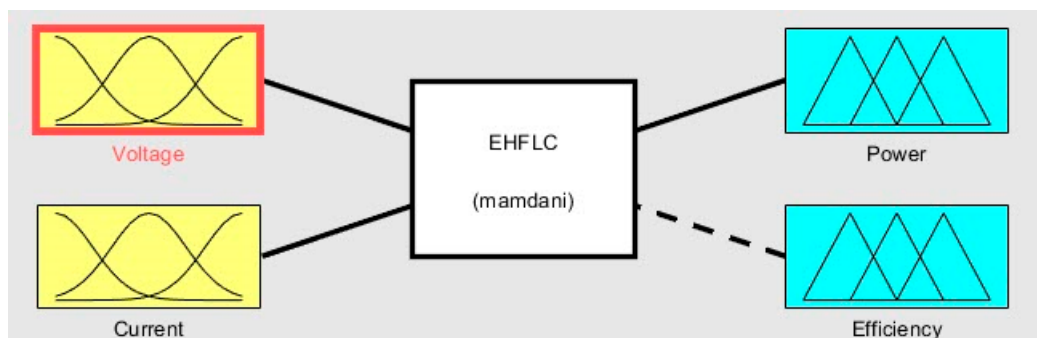


Figure 6. The energy harvester fuzzy logic controller (EHFLC).

After the simulation, the power 5.16 nano Watts with 0.363 efficiency has been obtained by taking the numerical value of voltage and current as 3.16 mV and 0.985 μ A, respectively. It is shown in the rule viewer in Figure 7.

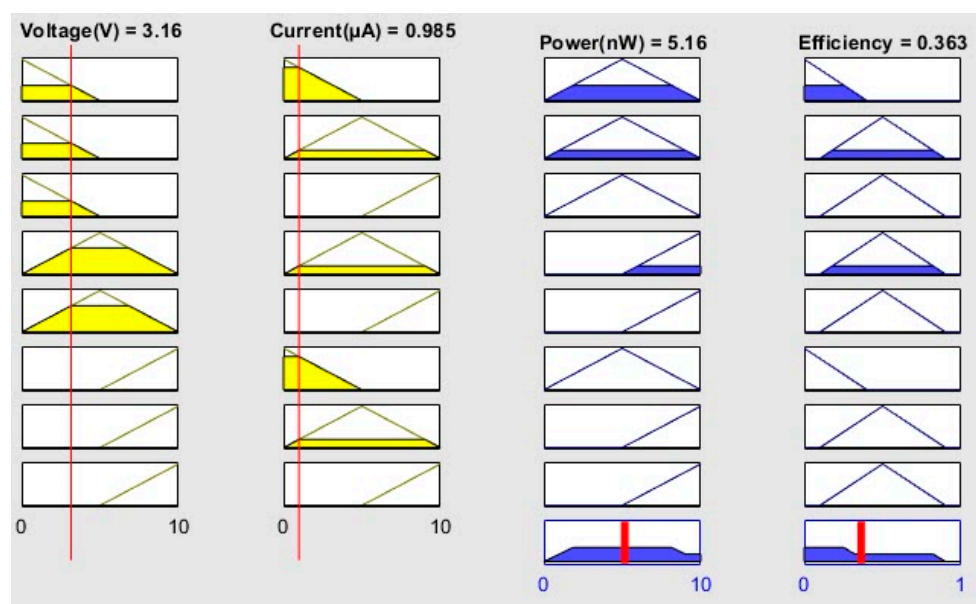


Figure 7. Rule Viewer of EHFLC.

The relationships between voltage, current, power, and efficiency are shown in the three-dimensional surface viewer graphs in Figure 8.

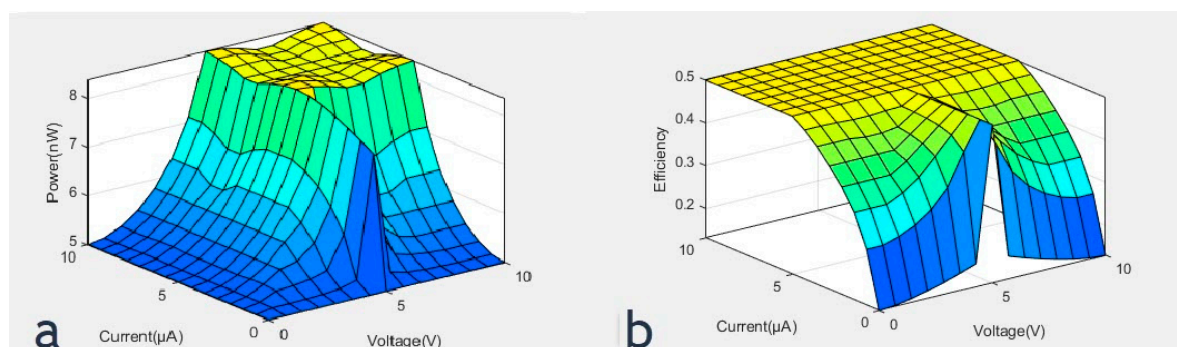


Figure 8. 3D graphs for EHFLC.

The 3D graphs in Figure 8 show how power and efficiency are dependent upon current and voltage. The variations in current and voltage lead to variations in power and efficiency. The fuzzy simulation shows that suitable power can be obtained from the EHFLC system and can be used for smart electronic devices. After simulation, a mathematical calculation has been performed to calculate the error. For the percentage error confirmation, Mamdani's formula was used for the mathematical calculations. It was found that the 5.17 nanoWatt power and 0.363 efficiency were obtained. The difference between the fuzzy simulated values and the Mamdani mathematical values is 0.01, with just 0.1% error.

4. Experimentation

All equipment and substrate were carefully cleaned using acetone and isopropyl alcohol (IPA). The aluminum substrates were washed with distilled water and acetone. Then they were cleaned by using IPA. It was then further electro-polished. After electropolishing, the substrates were sonicated in distilled water, ethanol, and acetone for 15 minutes, followed by air drying at 80 °C. The cleaned aluminum substrates were then subjected to self-designed anodization setup for the growth of nano pores template and further treated in a chemical bath for the growth of nano rods. Both setups are shown in Figure 9.

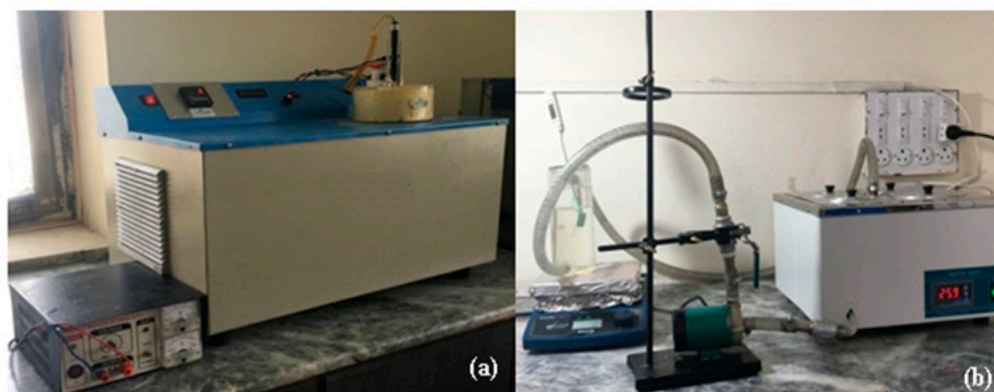


Figure 9. Self-designed setups (a) anodization (b) chemical bath deposition.

The first step is the mild anodization. In this step, 0.4 M oxalic acid solution was used as an electrolyte, the aluminum substrate was used as the anode, and a lead rod is used as a cathode. The first step was carried out at 38 V for 20 min. The voltage was gradually increased to 120 V. The anodization at 120 V was carried out for 15 minutes. The prepared sample was then etched using 4% phosphoric and chromic acid for 20 min at 80 °C. In step 2, hard anodization was performed. The electrolyte and

the cathode were the same as in the mild anodization; however, the process was carried out at 110 V for 4 h. The barrier layer formed was removed by changing the electrolyte to 0.3 M KCl and applying a opposite polarity voltage for 6 minutes. The prepared sample after step 2 of the anodization was etched in mercuric chloride solution for 15 min to remove all the impurities. The prepared anodized aluminum oxide membrane was coated with gold.

The porous gold coated membrane was first dipped in dodecanthiol solution for growth and sticking on ZnO nano rods for 2 h followed by drying at 60–70 °C. The solution was prepared by adding 1 mL of dodecanthiol in 100 mL of ethanol. The solution was stirred until a homogeneous mixture was created. The porous membrane was dipped. Then nano-rods were grown on the substrate using a self-designed chemical bath deposition set-up. Then, 20 mM solution of zinc acetate di-hydrate and hexa-amine was prepared in DI water. The porous membrane already dipped in dodecanthiol solution was inserted into the chemical bath deposition setup. The nano-rods were grown on the substrate for 6 hours at 95 °C. After the deposition process, the samples were washed using D.I water and followed by annealing at 400 °C. The process schematic is shown in Figure 10. It was further gold sputtered to form the electrode followed by testing.

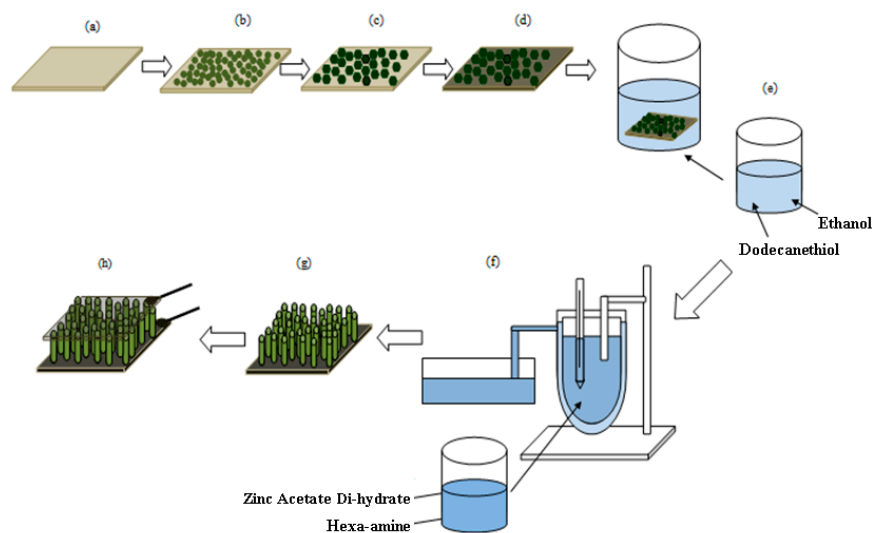


Figure 10. (a) The aluminum substrate; (b) the porous membrane formed after 1st step of anodization (mild anodization); (c) the porous membrane formed after the 2nd step of anodization (hard anodization); (d) the gold coating; (e) dipping in 1% dodecanthiol solution; (f) growth on the ZnO rods in the chemical bath; (g) ZnO nano rods on the AAO template; (h) sputtered gold electrodes.

5. Characterization and Testing

The surfaces of the AAO template and ZnO nanostructure were characterized to study morphology, optical, and electrical properties. The phase purity was studied using X-ray diffraction. The morphology and size of the prepared porous membrane and nano-rods were studied using scanning electron microscopy. The absorption band-gap was studied using a UV-Vis spectrophotometer. Similarly, the voltage and current outputs of the prepared film were studied using a self-designed cam follower setup shown in Figure 8 and attached with a SIGLENT SDS 1052DL digital storage oscilloscope. The pear-shaped cam follower setup consists of a frequency control VS Mini J7 and a rotating shaft with a movable stage and a fixed stage. The shaft is directly connected with the controller, which means that with an increase in frequency the shaft's rotation increases. The piezoelectric harvester is packed with a thin plastic layer and placed in between the two stages. The pulsating movement of shaft results in a force applied on the piezoelectric harvester in the d_{33} direction. The outputs of the harvester are attached in a series-parallel combination along with a bridge circuit. The output voltage and current can be seen on the screen of the SIGLENT SDS 1052DL digital storage oscilloscope and can be connected to a computer for analysis. The testing setup is shown in Figure 11.

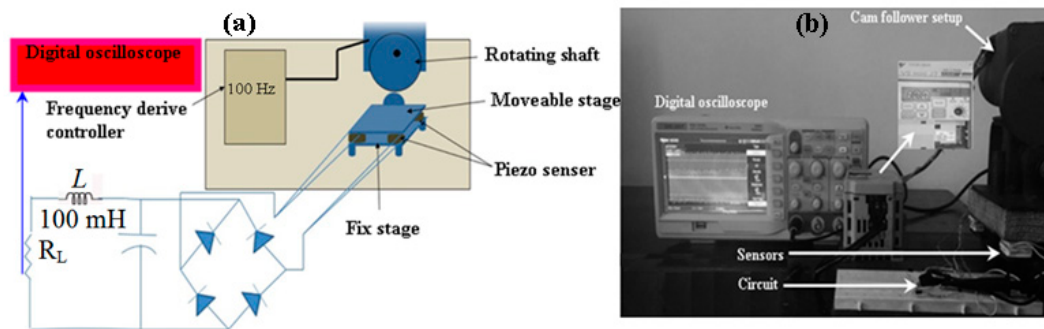


Figure 11. The self-designed cam follower Piezo harvester testing setup. (a) The schematic; (b) the experimental setup.

The structural morphology of the aluminum anodic oxide nano-porous template was studied using field emission scanning electron microscopy (FE-SEM). Figure 12 shows FE-SEM images of the AAO nano-porous template with and without sputtered gold coating.

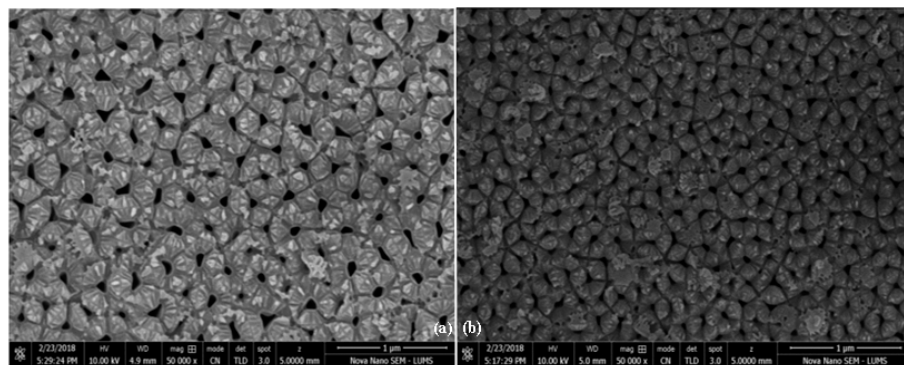


Figure 12. FE-SEM micrographs of the AAO nano-porous membrane (a) without gold sputtering (b) with gold sputtering.

The image revealed a structure that was highly ordered, uniform, and which contained an even layer of nano-pores. The pores have an aspect ratio of 500–800. The diameter of the nano-pores was in the range of 80 nm. The phase purity of ZnO nano-rods fabricated using chemical bath deposition on an anodized aluminum oxide substrate was studied using X-ray diffraction (XRD). The XRD pattern shown in Figure 13 of ZnO nano-rods prepared on AAO substrate shows distinctive peaks at $2\theta = 31.73^\circ$, 34.41° , 47.51° , 54.58° , and 69.85° , which can be assigned to (100), (101), (111), (311) and (220) planes respectively, with a hexagonal ZnO crystal structure.

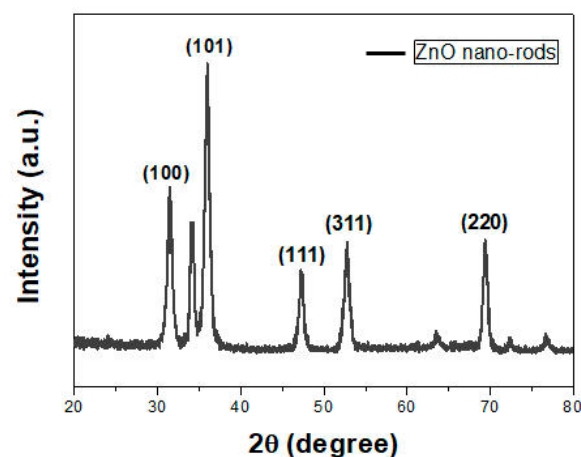


Figure 13. The X-ray diffraction pattern of ZnO nano-rods deposited on the AAO template.

The SEM micrographs of the ZnO rods are shown in Figure 14 and show the smooth growth of ZnO nanorods on the AAO substrate. The periodic arrangements on the ZnO nano-rods orderly spread in an orderly way with great uniformity.

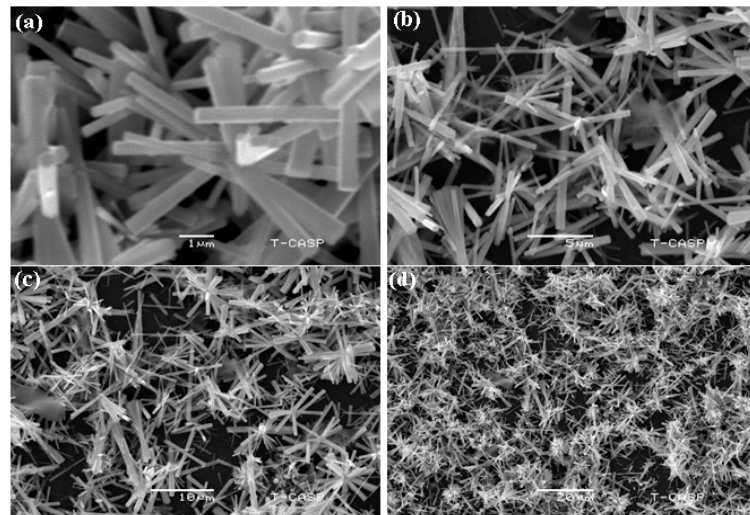


Figure 14. SEM of ZnO nano-rods deposited on the AAO template. (a) 1 μm ; (b) 5 μm ; (c) 10 μm ; (d) 20 μm .

The optical properties of the prepared ZnO nano-rods array deposited on the AAO template were studied to analyze the band-gap of the prepared material from wavelengths ranging from 300–1100 nm. The absorption coefficient was 390 nm, calculated by the tangential fitting of the linear portion of the spectrum as shown in Figure 15. Called cut-off wavelength, it gives the onset wavelength of light that is absorbed. Using the graph between absorption and wavelength, E_g (band-gap) was calculated using transmittance, $\%T = (\log_{10}^{-A})/100$, where A is the absorbance. $E_g = 1240/\lambda$ (nm), where λ is the wavelength, and E_g (eV) is the band-gap. The absorption coefficient was calculated using $\alpha = 1/t \ln(1/\%T)$, where $\%T$ is the % transmittance of the solution. The band-gap was calculated to be 3.22 eV.

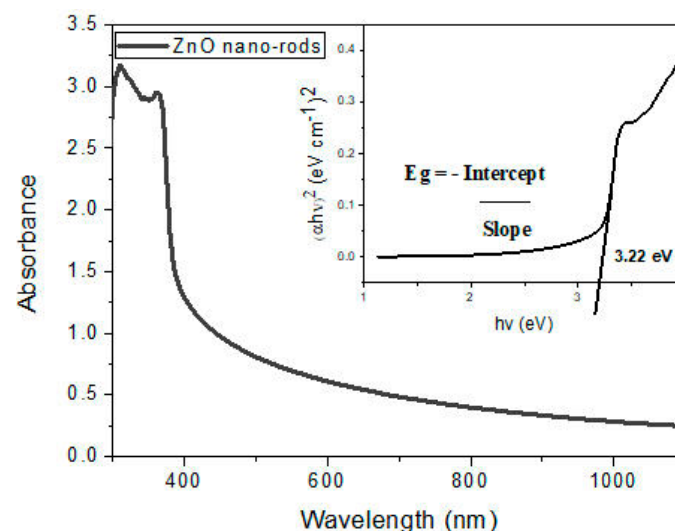


Figure 15. The absorption spectrum of ZnO nanorods and Tauc plot extracted from the absorption spectrum.

For piezoelectric generators, the mechanical resonance frequency is the required frequency at which the optimum power is harvested. However, in a condition when excitation vibrational

frequencies are different from the resonance frequency, then the generator would not generate the optimum power output. In such conditions, power generation is enhanced using the impedance load matching technique. To achieve such a state, the impedance of the piezoelectric generator is matched with a load circuit so that the maximum power is transferred to the load. This impedance matching was achieved using an energy harvesting circuit. The piezoelectric properties of the prepared piezoelectric generator with an effective area of 4 cm were studied by applying a cyclic force. The open circuit voltage was measured with both the polarities and was found to be in the range of 3–6.4 mV. Similarly, the short circuit current was also measured in the range of 0.45–1.5 μA in both the polarities. These results are shown below in Figures 16 and 17.

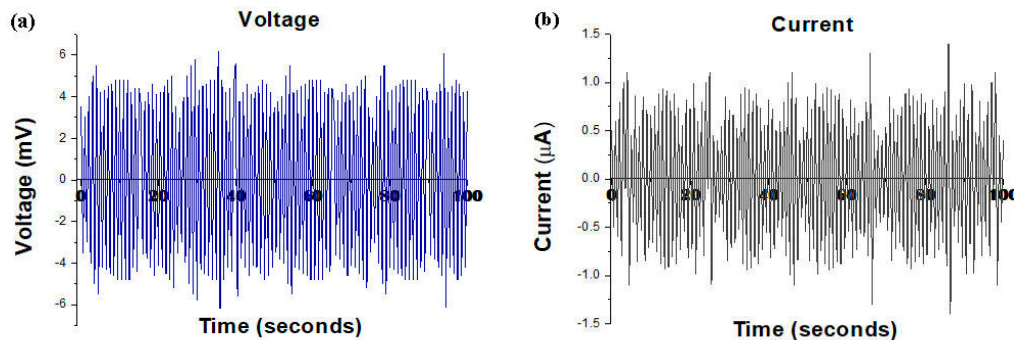


Figure 16. For 100 seconds: (a) Open circuit voltage; (b) short circuit current.

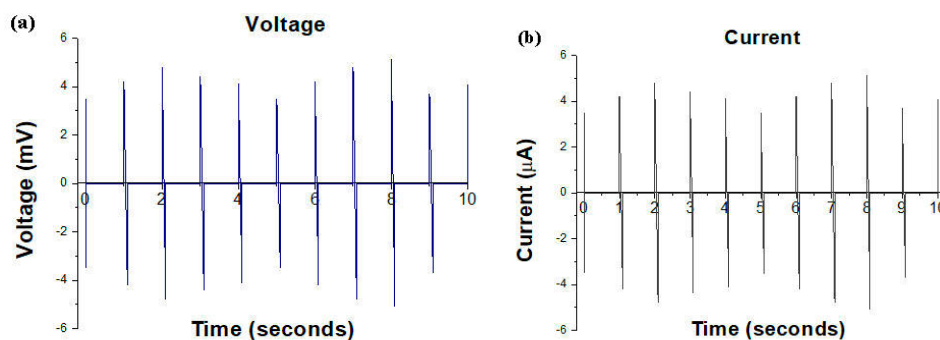


Figure 17. For 10 seconds: (a) Open circuit voltage; (b) short circuit current.

The output of the MEMS energy harvester depends upon various factors like the growth of the vertically aligned nanostructure, material properties, cyclic force contact angle, harvesting methods, and the impedance matching circuit. In literature the various energy harvester, maximum power at the output can be obtained by adding load with matched impedance to source and load. The impedance matching has been obtained by using the maximum power transfer theorem. As piezoelectric generators act like capacitive circuits, reactive and resistive loads were used for impedance matching [44]. In piezoelectric generators, resonance frequency with mechanical mode was needed frequency where highest power can be harvested. When resonant frequency do not matched with excitation frequency, then no output would be obtained from the generator. In such a condition, the power generation can be boosted by using load with matching method of impedance [45]. This impedance matching was achieved by using circuits such as bridge circuits or DC-DC buck converters attached to the energy harvester circuit. The internal series resistance of the prepared ZnO based nano-harvester was calculated by J-V characteristics.

The slope of the non-linear curve provides the value of internal series resistance. The increase in R_s leads to increases in the I_2R_s and power losses which decrease the power density and V_{oc} . Similarly, increased R_s caused the decrease in J_{sc} of the device, and consequently the efficiency reduced for system. The internal series resistance of the prepared system was 0.022 k Ω . For impedance matching,

the output of the piezoelectric sensor subjected to pressure using a cam follower setup was connected to a bridge circuit, as shown in Figure 11. For an efficient energy harvesting system, the attached load was matched with the internal resistance, i.e., 0.022 k Ω of the energy harvester. The inductor was tuned to match the internal resistance [46] of the piezoelectric source so that maximum power output can be achieved.

6. Conclusions

In summary, a small piezoelectric energy harvester was mechanically and physically studied for a smart MEMS system. The harvester was a combination of ZnO nano-rods fabricated on an anodized aluminum oxide template with accurate patterned growth of the nanostructures. The anodized aluminum oxide template featuring 80 nm pore-sizes was synthesized and ANSYS simulation predicted that by applying force, stress is produced on the template under the elastic limit. A uniform array of ZnO nano-rods was grown on AAO and the optical study shows that a band-gap of 3.22 eV was measured. The piezoelectric property was studied by using a self-designed cam follower setup with a harvester effective area of 4 cm by applying a cyclic force using a variable frequency controller. The open circuit voltage and short circuit current were measured with both the polarities and were found to be in the range of 3–6.4 mV and 0.45–1.5 μ A, respectively. The power of 5.16 nW has been obtained by taking the numerical value of the voltage (V_{oc}) and current (I_{sc}) as 3.16 mV and 0.985 μ A, respectively, in the fuzzy logic MATLAB simulation. The impedance of the piezoelectric generator is matched with a load circuit for the maximum power transfer. By connecting these harvesters in a series-parallel combination, the overall current and voltage can be enhanced for further use in large scale energy harvesting.

Author Contributions: B.A. performed the current study. M.W.A. gave ideas, technical help and guidance throughout the study. S.T. contributed to the simulation.

Funding: This research received no external funding. This study was conducted in Nano Electronics Research Lab., GC University Lahore, Pakistan.

Conflicts of Interest: The authors declare no conflict of interest.

References

1. Sivanandam, S.; Sumathi, S.; Deepa, S. *Introduction to Fuzzy Logic Using MATLAB*; Springer: Berlin, Germany, 2007; Volume 1.
2. Chen, C.Y.; Liu, T.H.; Zhou, Y.; Zhang, Y.; Chueh, Y.L.; Chu, Y.H.; He, J.R.; Wang, Z.L. Electricity generation based on vertically aligned PbZr_{0.2}Ti_{0.8}O₃ nano-wires arrays. *Nano-Energy* **2012**, *1*, 424–428. [[CrossRef](#)]
3. Khan, S.A.; Afzulpurkar, N.V.; Bodhale, D. A Facile, Cost Effective, Patterned ZnO Microwires Synthesis for Large-Scale Fabrication of Piezo-electric generators. *Nanosci. Nano-Technol. Lett.* **2015**, *7*, 1–7.
4. Liao, Q.; Zhang, Z.; Zhang, X.; Mohr, M.; Zhang, Y.; Fecht, H. Flexible piezoelectric nanogenerators based on a fiber/ZnO nanowires/paper hybrid structure for energy harvesting. *Nano Res.* **2014**, *7*, 917–928. [[CrossRef](#)]
5. Opoku, C.; Dahiya, A.S.; Oshman, C.; Caryel, F.; Vittrant, G.; Alquier, D.; Camara, N. Fabrication of ZnO Nanowire Based Piezoelectric Generators and Related Structures. *Phys. Procedia* **2015**, *70*, 858–862. [[CrossRef](#)]
6. Gao, P.; Song, J.; Liu, J.; Wang, Z. Nanowire Piezoelectric Nanogenerators on Plastic Substrates as Flexible Power Sources for Nanodevices. *Adv. Mater.* **2007**, *19*, 67–72. [[CrossRef](#)]
7. Qiu, Y.; Zhang, H.; Hu, L.; Wang, L.; Wang, B.; Ji, J.; Liu, Q.; Liu, X.; Lin, J.; Li, F.; Han, S. Nanoscale Flexible piezoelectric nanogenerators based on ZnO nanorods grown on common paper substrates. *Nanoscale* **2012**, *4*, 6568–6573. [[CrossRef](#)] [[PubMed](#)]
8. Riaz, B.M.; Song, J.; Nur, O.; Wang, Z.L.; Willander, M. Study of the Piezoelectric Power Generation of ZnO Nanowire Arrays Grown by Different Methods. *Adv. Fundam. Mater.* **2011**, *21*, 628–633. [[CrossRef](#)]
9. Ou, C.; Sanchez-Jimenez, P.E.; Datta, A.; Boughhey, F.L.; Whiter, R.A.; Sahonta, S.L.; Kar-Narayan, S. ‘Template-Assisted Hydrothermal Growth of Aligned Zinc Oxide Nanowires for Piezoelectric Energy Harvesting Applications. *ACS Appl. Mater. Interfaces* **2016**, *8*, 13678–13683. [[CrossRef](#)] [[PubMed](#)]

10. Zhu, G.; Yang, R.; Wang, S.; Wang, Z.L. Flexible High-Output Nanogenerator Based on Lateral ZnO Nanowire Array. *Nano-Lett.* **2010**, *10*, 3151–3155. [[CrossRef](#)] [[PubMed](#)]
11. Meninger, S.; Murinda, J.O.M.; Amirtharajah, R.; Chandrakasan, A.P.; Lang, J.H. Vibration to Electric Energy Conversion. *IEEE Trans. VLSI Syst.* **2001**, *9*, 64–76. [[CrossRef](#)]
12. Hu, Y.; Chen, X.; Zhang, Y.; Lin, L.; Snyder, R.L.; Wang, Z.L. A nano-generator for energy harvesting from a rotating tire and its application as a self-powered pressure/speed sensor. *Adv. Mater.* **2011**, *23*, 4068–4071. [[CrossRef](#)] [[PubMed](#)]
13. Beeby, S.B.; Tudor, M.J.; White, N.M. Energy harvesting vibration sources for microsystems applications. *Meas. Sci. Technol.* **2006**, *17*, 175–195. [[CrossRef](#)]
14. Agarwal, R.; Peng, B.; Espinosa, H.D. Experimental—Computational Investigation of ZnO nanowires Strength and Fractures. *Nano-Lett.* **2009**, *9*, 4177–4183. [[CrossRef](#)] [[PubMed](#)]
15. Wang, J.; Kulkarni, A.J.; Ke, F.J.; Bai, Y.J.; Zhou, M. Novel Mechanical behaviour of ZnO nano-rods. *Comput. Methods Appl. Mech. Eng.* **2008**, *197*, 3182–3189. [[CrossRef](#)]
16. Baruah, S.; Thanachayanont, C.; Dutta, J. Growth of ZnO nano-wires on non-woven polyethylene fibers. *Sci. Technol. Adv. Mater.* **2008**, *9*, 025009. [[CrossRef](#)] [[PubMed](#)]
17. Hsueh, T.J.; Hsu, C.L.; Chang, S.J.; Chen, I.C. Laterally Grown ZnO nano-wires ethanol gas-sensor. *Sens. Actuators B* **2007**, *126*, 473–477. [[CrossRef](#)]
18. Kumar, B.; Kim, S.W. Energy harvesting based on semi-conductor piezo-electric ZnO nano-structures. *Nano-Energy* **2012**, *1*, 342–355. [[CrossRef](#)]
19. Yu, A.; Li, H.; Tang, H.; Liu, T.; Jiang, P.; Wang, Z.L. Vertically integrated nanogenerator based on ZnO nano-wires array. *Phys. Status Solidi RRL* **2011**, *4*, 162–164. [[CrossRef](#)]
20. Lepot, N.; Bael, M.K.V.; Rul, H.V.D.; Haen, J.D.; Peeters, R.; Franco, D.; Mullens, J. Synthesis of ZnO nano-rods from aqueous solution. *Mater. Lett.* **2007**, *61*, 2624–2627. [[CrossRef](#)]
21. Ni, Y.N.; Wei, X.W.; Hong, J.M.; Ye, Y. Hydrothermal preparation and optical properties of ZnO nano-rods. *Mater. Sci. Eng. B* **2005**, *121*, 42–47. [[CrossRef](#)]
22. Xu, S.; Wang, Z.L. One dimensional ZnO nano-structures: Solution growth and functional properties. *Nano Res.* **2011**, *4*, 1013–1098. [[CrossRef](#)]
23. Xu, S.; Lao, C.; Weintraub, B.; Wang, Z.L. Density controlled growth of aligned nanowires arrays by seedless chemical approach on smooth surfaces. *J. Mater. Res.* **2008**, *23*, 2072–2077. [[CrossRef](#)]
24. Afzal, M.J.; Ashraf, M.W.; Tayyaba, S.; Hossain, M.K.; Afzulpurkar, N. Sinusoidal Microchannel with Descending Curves for Varicose Veins Implantation. *Micromachines* **2018**, *9*, 59. [[CrossRef](#)] [[PubMed](#)]
25. Afzal, M.J.; Tayyaba, S.; Ashraf, M.W.; Hossain, M.K.; Uddin, M.J.; Afzulpurkar, N. Simulation, Fabrication and Analysis of Silver Based Ascending Sinusoidal Microchannel (ASMC) for Implant of Varicose Veins. *Micromachines* **2017**, *8*, 278. [[CrossRef](#)] [[PubMed](#)]
26. Dey, B.; Hossain, A.; Ballas, V.E.; Bera, R.N. Improved Energy Detector for Spectrum Sensing Using Neuro-Fuzzy Double Threshold Technique. *Studies Inform. Control* **2017**, *3*, 335–342. [[CrossRef](#)]
27. Tariq, M.I. Agent Based Information Security Framework for Hybrid Cloud Computing. *KSII Trans. Internet Inf. Syst.* **2019**, *13*, 406–434.
28. Kim, J.-Y.; Kim, H.-M.; Kim, S.-K.; Jeon, J.-H.; Choi, H.-K. Designing an energy storage system fuzzy PID controller for microgrid islanded operation. *Energies* **2011**, *4*, 1443–1460. [[CrossRef](#)]
29. Hou, X.; Sun, Y.; Yuan, W.; Han, H.; Zhong, C.; Guerrero, J.M. Conventional P- ω /QV droop control in highly resistive line of low-voltage converter-based ac microgrid. *Energies* **2016**, *9*, 943. [[CrossRef](#)]
30. Liu, C.-L.; Chen, J.-H.; Liu, Y.-H.; Yang, Z.-Z. An asymmetrical fuzzy-logic-control-based MPPT algorithm for photovoltaic systems. *Energies* **2014**, *7*, 2177–2193. [[CrossRef](#)]
31. Umair Ali, M.; Hussain Nengroo, S.; Adil Khan, M.; Zeb, K.; Ahmad Kamran, M.; Kim, H.-J. A real-time simulink interfaced fast-charging methodology of lithium-ion batteries under temperature feedback with fuzzy logic control. *Energies* **2018**, *11*, 1122. [[CrossRef](#)]
32. Cheng, Y.-S.; Liu, Y.-H.; Hesse, H.C.; Naumann, M.; Truong, C.N.; Jossen, A. A PSO-Optimized Fuzzy Logic Control-Based Charging Method for Individual Household Battery Storage Systems within a Community. *Energies* **2018**, *11*, 469. [[CrossRef](#)]
33. Yuan, Y.; Zhang, T.; Shen, B.; Yan, X.; Long, T. A Fuzzy Logic Energy Management Strategy for a Photovoltaic/Diesel/Battery Hybrid Ship Based on Experimental Database. *Energies* **2018**, *11*, 2211. [[CrossRef](#)]

34. Li, Z.; Zhou, G.; Zhu, Z.; Li, W. A study on the power generation capacity of piezoelectric energy harvesters with different fixation modes and adjustment methods. *Energies* **2016**, *9*, 98. [[CrossRef](#)]
35. Liu, Z.; Wang, X.; Zhang, R.; Wang, L. A dimensionless parameter analysis of a cylindrical tube electromagnetic vibration energy harvester and its oscillator nonlinearity effect. *Energies* **2018**, *11*, 1653. [[CrossRef](#)]
36. An, X.; Song, B.; Mao, Z.; Ma, C. Layout Optimization Design of Two Vortex Induced Piezoelectric Energy Converters (VIPECs) Using the Combined Kriging Surrogate Model and Particle Swarm Optimization Method. *Energies* **2018**, *11*, 2069. [[CrossRef](#)]
37. Zhang, R.; Wang, X.; John, S. A comprehensive review of the techniques on regenerative shock absorber systems. *Energies* **2018**, *11*, 1167. [[CrossRef](#)]
38. Varadarajan, E.; Bhanusri, M. Design and simulation of unimorph piezoelectric energy harvesting system. In Proceedings of the COMSOL Conference, Bengaluru, India, 17 October 2013; pp. 17–18.
39. Sabaawi, A.M.; Tsimenidis, C.C.; Sharif, B.S. Infra-red nano-antennas for solar energy collection. In Proceedings of the 2011 Loughborough Antennas and Propagation Conference (LAPC), Loughborough, UK, 14–15 November 2011; pp. 1–4.
40. Genovese, A.; Strano, S.; Terzo, M. Model-based study of a resonant system in a railway air spring secondary suspension for energy harvesting applications. In Proceedings of the 2018 2nd International Conference on Mechatronics Systems and Control Engineering, Amsterdam, The Netherlands, 21–23 February 2018; ACM: New York, NY, USA, 2018; pp. 45–51.
41. Pasharavesh, A.; Ahmadian, M.T. Analytical and numerical simulations of energy harvesting using MEMS devices operating in nonlinear regime. *Eur. Phys. J. B* **2018**, *91*, 241. [[CrossRef](#)]
42. Ennawaoui, C.; Lifi, H.; Hajjaji, A.; Elballouti, A.; Laasri, S.; Azim, A. Mathematical modeling of mass spring's system: Hybrid speed bumps application for mechanical energy harvesting. *Eng. Solid Mech.* **2019**, *7*, 47–58. [[CrossRef](#)]
43. Xu, M.; Zhao, T.; Wang, C.; Zhang, S.L.; Li, Z.; Pan, X.; Wang, Z.L. High Power Density Tower-like Triboelectric Nanogenerator for Harvesting Arbitrary Directional Water Wave Energy. *ACS Nano* **2019**. [[CrossRef](#)] [[PubMed](#)]
44. Bakshi, A.V.B.U.A. *Network Analysis and Synthesis*; Technical Publications: Maharashtra, India, 2009.
45. Saggini, S.; Giro, S.; Ongaro, F.; Mattavelli, P. Implementation of Reactive and Resistive Load Matching for Optimal Energy Harvesting from Piezoelectric Generators. In Proceedings of the 2010 IEEE 12th Workshop on Control and Modeling for Power Electronics (COMPEL), Boulder, CO, USA, 28–30 June 2010; pp. 1–6.
46. Kim, H.; Priya, S.; Stephanou, H.; Uchino, K. Consideration of Impedance Matching Techniques for Efficient Piezoelectric Energy Harvesting. *IEEE Trans. Ultrason. Ferroelectr. Freq. Control* **2007**, *54*, 1851–1859. [[CrossRef](#)] [[PubMed](#)]



© 2019 by the authors. Licensee MDPI, Basel, Switzerland. This article is an open access article distributed under the terms and conditions of the Creative Commons Attribution (CC BY) license (<http://creativecommons.org/licenses/by/4.0/>).